EFFECTS OF ROTOR SKEW ANGLE ON FLUX SWITCHING PERMANENT MAGNET (FSPM) MACHINES CHARACTERISTICS

[1]Mostafa. AHMADI DARMANI [2]Seyyed Mehdi. MIRIMANI [3]Fabrizio. MARIGNETTI

1. Faculty of Electrical and Computer Engineering, Science and Research Branch, Islamic Azad University
Tehran, Iran, Phone: +989121382532, Email: mostafa.ahmadi.d@gmail.com
2. Faculty of Electrical and Computer Engineering, Babol University of Technology
Babol, Iran, Phone: +989112141856, Email: mirimani@nit.ac.ir
3. Department of Electrical Engineering, University of Cassino and Southern Lazio
Cassino, Italy, Phone +3907762993716, Email: marignetti@unicas.it

Abstract— *Not only does rotor skewing as a cost-effective technique reduce the cogging torque, but also it affects machines performance too. Hence, this paper studies the torque, back-EMF and loss characteristic of a Flux Switching Permanent Magnet (FSPM) machine with rotor skewing. The cogging torque, torque profile, induced EMF and iron core losses of a 10/12 FSPM machine with various degrees of rotor skewing are calculated and compared using three dimensional finite element analysis. First and foremost, the results have shown that the torque oscillation is totally eliminated when skew angle is equal to 6 degrees. In addition, the peak value of both output torque and back-EMF does not change significantly, and they reduce at most 5%. Finally, the influences of rotor skewing on the iron core losses are carried out using Bertotti formula and it is discovered that by increasing the skew angle, core losses almost do not vary.*

Key words: *Flux Switching Permanent Magnet Machines, Cogging Torque, Rotor Skewing, Finite Element Analysis, Torque Profile, Back-EMF Characteristics, Core Losses*

1. Introduction

The electrical machines which have permanent magnets (PMs) in their structure are able to produce higher torque density and efficiency in comparison with other conventional types [1]. Among PM machines, stator-PM machines achieve higher power density if compared to rotor-PM machines because the PMs are well-ventilated. In addition, stator-PM machines have better mechanical reliability for high-speed applications as their windings are placed in the stator [2]. Stator-PM machines are consisted to three categories, Doubly Salient Permanent Magnet (DSPM) machines, Flux Reversal Permanent Magnet (FRPM) machines and Flux Switching Permanent Magnet (FSPM) machines [3]. FSPM machines have the highest power density among other types, because of the highest air-gap flux density which is caused by the flux concentration effect. In addition, they enjoy high power density, torque density, high flux-weakening capability and robust structure [3]-[4]. These types of electrical machines are a suitable candidate for both low-speed and high-speed application such as starter-generator in aircraft [5], hybrid vehicles [6] and wind turbines [7]. The recent literature has focused mainly on design optimization [8]-[9], on the enhancement of the topology and on the performance analysis of FSPM machines [10]. Most researches have been focused on design procedure, optimized design and performance analysis [11] while the cogging torque has not been studied properly. In general, cogging torque in flux switching machines is higher than in other machines and it generates unpleasant vibration and acoustic noise. In order to obtain high performance, the minimization of torque oscillations consists substantially upon the effort to constant the alignment between the rotor teeth and the permanent magnets [12]. Rotor/stator skewing is one of the common methods to reduce the pulsation of the cogging torque [13]. Rotor skewing in FSPM machines is way easier in comparison with stator skewing because of segmented construction of stator and embedded PMs in stator structure.

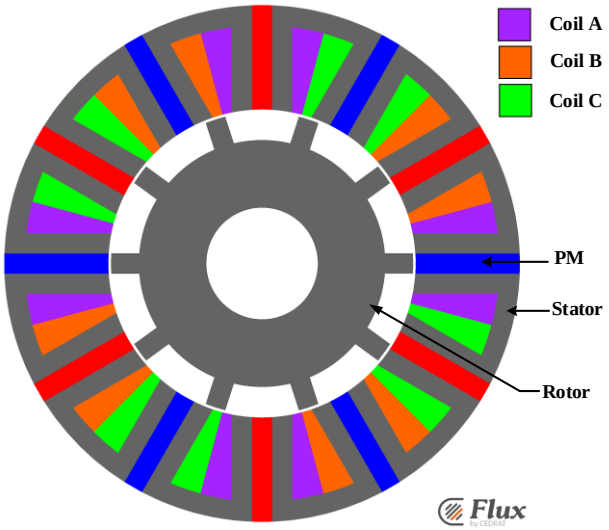

Fig. 1. Schematic of proposed FSPM machine

Not only does rotor skewing have influence on the cogging toque, but it also affects other parameters of the machine which have direct impact on machine performance such as output torque, back-EMF and core

losses which are missed in other literatures. The objective of this paper is to explore the effects of rotor skewing in FSPM machines for performance prediction of the FSPM machines. Moreover, it proves crucial to model the machine accurately, therefore Finite Element Analysis (FEA) is performed to analyze various values of the rotor skewing in a prototype FSPM machine.

2. Finite element simulation

The studied FSPM machine is a three-phase 12/10 motor. The 2D schematic of proposed FSPM machine is shown in Fig. 1.

The main geometric parameters of the machine are given in Table 1.

The FSPM machine is modeled with the CEDRAT Flux package which is a FE software. The machine has concentrated winding in which all coils are connected in series and supplied by three-phase sinusoidal current source. The circuit is coupled to the magnetic domain in this study.

Table 1. Major Parameters of FSPM Machine

Quantity	Value
Stator pole numbers	12
Rotor pole numbers	10
Outer diameter of stator	90mm
Active axial length	25mm
Air-gap length	0.5mm
Rotor pole width	4mm
Outer diameter of rotor	55mm
PM thickness	3.6mm
Stator tooth width	3.6mm
Stator back iron thickness	3.6mm
Number of turns per phase	72
Rated current	14A
Speed	400rpm

The periods of the cogging torque during a stator slot pitch is given as follows [14]:

$$N_p = \frac{N_r}{GCD(N_s.N_r)} \quad (1)$$

where GCD(Ns,Nr) is the greatest common divisor between the rotor pole number Nr and the stator pole number Ns. For the studied machine, GCD(10,12) and Np are 2 and 5 respectively. Thus, the suitable skew angle to reduce the cogging torque is between 0 to θskew and can be achieved as follows [14]-[15]:

$$\theta_{skew} = \frac{360}{N_p N_s} \quad (2)$$

In order to model various condition of rotor skewing completely, the parameter θ_{skew} i.e. the skew angle is varied in six steps. A skewed model of the proposed FSPM machine is shown in Fig. 2 for θ_{skew}=6°. Moreover, the flux distribution of skewed FSPM machine for both rotor and stator shows in Fig. 3 (a) and (b) respectively.

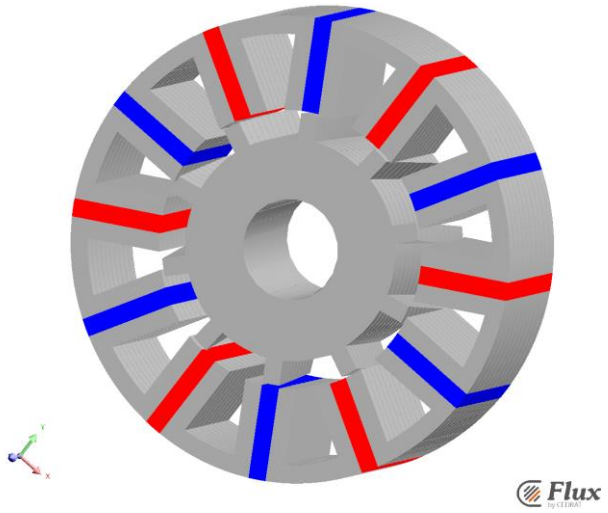

Fig. 2. Schematic representation of skewed FSPM machine

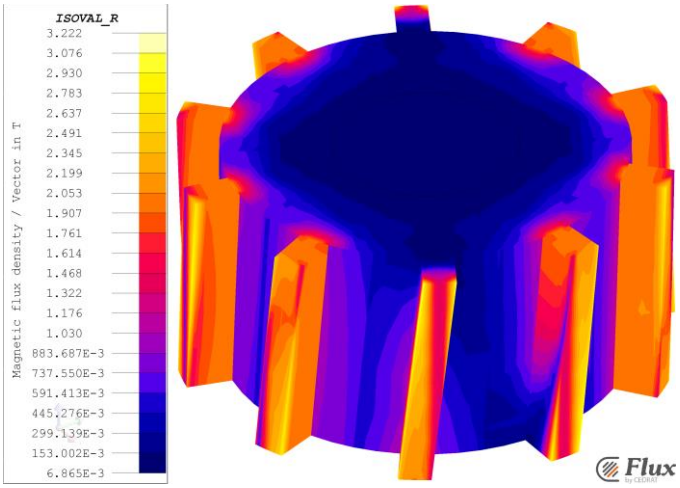

(a)

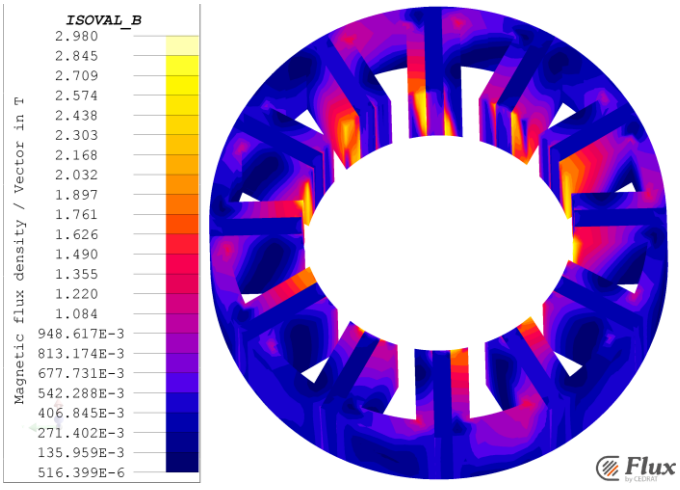

(b)

Fig. 3. Flux disturbution of skewed FSPM machine, a): Rotor, b): Stator

3. Cogging torque in FSPM

The cogging torque is produced by the interaction between the stator PMs and the rotor salient poles on open-circuit. In other words, the variation of energy in a machine while its rotor is rotating causes to generate a periodic torque pulsation even if the current is equal to zero due to the rotor field tends to be aligned with the stator poles.

Generally, total co-energy in an electrical machine consists of three terms which are corresponded to of the self-inductance, permanent magnet and that due to mutual flux. In an FSPM machine, total co-energy can be calculated as follow:

$$W_{co} = \frac{1}{2}Li^2 + \frac{1}{2}\mathcal{R}\varphi_{PM}^2 + Ni\varphi_{PM} \tag{3}$$

where L is the machine inductance, i is the current of the machine, $\mathcal{R}$ is total reluctance which is seen by the magneto-motive force source and the magnetic field, φ_{PM} is the magnetic flux of the permanent magnet and N is the number of stator winding. Also the electromagnetic torque can be derived estimated as follows:

$$T = -\frac{\partial W_{co}}{\partial \beta} \tag{4}$$

where β is the angular position of rotor. The total energy of the machine can be calculated as follow:

$$T_{cog} = -\frac{\partial W_{co}}{\partial \beta}\Big|_{i=constant} \tag{5}$$

$$T_{cog} = -\frac{1}{2}\varphi_{PM}^2 \frac{d\mathcal{R}}{d\beta} \tag{6}$$

When the permeability of the iron core is extremely large in compare with the permeability of the air-gap and PMs and the variation of energy in the iron core is neglected, co-energy is almost equal to stored energy in the air-gap. The stored energy in the air-gap can be calculated as follow:

$$W_{co} \approx W_{air-gap} \tag{7}$$

$$W_{air-gap} = \frac{1}{2\mu_0}\int_V B^2(\alpha)dV = \frac{1}{2\mu_0}\int_V B^2(\alpha)G^2(\alpha,\beta)dV \tag{8}$$

where α the angle along the circumference of the air-gap, B(α) is the distribution of the air-gap flux density along the perimeter, G(α,β) is a function used to model the effect of the salient rotor [14].

Fourier expansion of $B^2(\alpha)$ and $G^2(\alpha,\beta)$ are shown in equations (9) and (10) respectively.

$$B^2(\alpha) = B_0 + \sum_{n=1}^{\infty} B_n \cos(np_s\alpha) \tag{9}$$

$$G^2(\alpha,\theta) = G_0 + \sum_{m=1}^{\infty} G_n \cos(mp_r(\alpha+\beta)) \tag{10}$$

Substitution of (9) and (10) into (8) yield an expression for the cogging torque of an FSPM machine:

$$T_{cog}(\beta) = \frac{p_r l_{st}}{4\mu_0}\left(\frac{D_{si}^2 - D_{ro}^2}{4}\right)\sum_{n=1}^{\infty} nG_nB_{nk}\sin(k\beta) \tag{11}$$

where l_{st} is the stack length, D_{si} the inner diameter of stator, D_{ro} the outer diameter of rotor, μ_0 the permeability of the air and k the Least Common Multiple of the number of stator poles and the number of rotor poles. According to (7), the cogging torque are proportional to G_n times B_{nk}.

Fig, 4 shows the cogging torque of the studied machine for different skew angles. The results show that the cogging torque decreases considerably by increasing the skew angle. It is observed that with 6° rotor skewing, the cogging torque is around zero, causing the machine to have a smoother torque profile. In table II, the amount of cogging torque for various degree of skew angle is compared. It can be seen that cogging torque reduces around 99% in comparison to the condition that θ_{skew}=0°. It can be concluded that skewing the rotor is the best approach to eliminate the cogging torque. In addition, it is irrefutable that this method is easier if compared to other methods such as teeth pairing or tooth notching. Table II compare the cogging torque for various degree of skew angles.

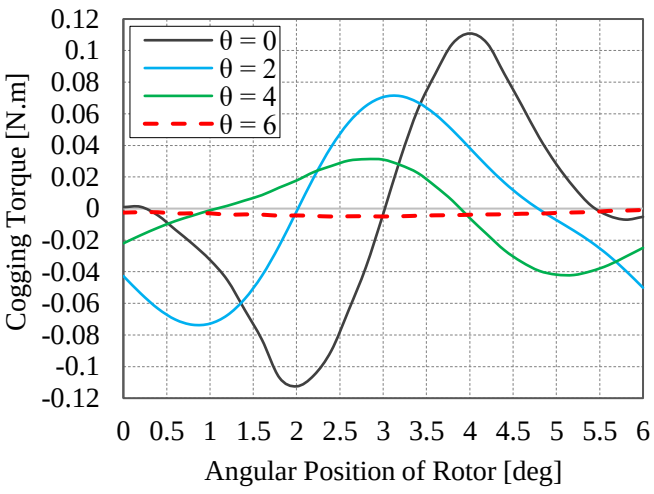

Fig. 4. FE computation of cogging torque for different values of skew angle

Table 2: Compare of cogging torque for various values of Skew angle

Skew Angle	T_{Cog} [N.m]	Cogging Torque Reduction [%]
0	0.110819	0.00%
1	0.102078	7.89%
2	0.07119	35.76%
3	0.04762	57.03%
4	0.031294	71.76%
5	0.013942	87.42%
6	0.00088	99.21%

4. Torque Characteristics

Generally, output torque of FSPM machines can be defined as:

$$T_{output} = \frac{P_{output}}{\omega} \tag{12}$$

$$P_{output} = \eta m \epsilon E I_a \cos(\varphi) \tag{13}$$

where P_{output} is output power and ω angular speed, η is the efficiency of the machine, m is the number of machine phases, ϵ is the ratio of the induced EMF by the stator PM flux at no-load E to the machine terminal voltage V, I_a is the phase current and cos(φ) is the power factor.

After applying rotor skewing in FSPM machines, the output torque can be expressed as:

$$T_{output} = \frac{\eta m \epsilon E I_a \cos(\varphi)}{\omega} \tag{14}$$

One of the vital characteristics of an electric machine is the output torque which can be affected by the skewing of the rotor. According to the technical literature, rotor/stator skewing causes electrical machines torque to drop [5].

In order to model the effect of rotor skewing on the machine torque, the coefficient k_{skew} is multiplied to equation (10) is calculated by FEA and it is expressed as:

$$T_{output} = k_{skew} \frac{\eta m \epsilon E I_a \cos(\varphi)}{\omega} \tag{15}$$

As shown in Fig. 5, the torque of the machine decreases by increasing the skew angle. At the first look, it seems that the machine's torque decreases to less than half, but in order to calculate the drop of the output torque we need to compute the maximum torque-phase angle profile (T-δ) for one cycle. To compute the T-δ, rated current I_a is injected to phase A, and $-I_a/2$ is injected to phase B and C. Fig. 6 shows the T-δ for different values of skew angle. As it can be seen in Fig. 6, the maximum torque drop is limited. Also, the decrement of maximum machine's torque versus θ_{skew} is presented in Fig. 7. Moreover, the maximum torque, its reduction and percentage of torque ripple is presented in table III. It can be observed that when $\theta_{skew}=6^{\circ}$, the maximum torque drops 5.5% while torque ripple reduces 5.38%.

5. Back-EMF Characteristics

Back-EMF plays a significant role in machines performance, and a small change in this parameter affects machine's performance.

According to Faraday's induction law, the voltages induced in the windings of a skewed rotor machine can be determined as:

$$E = -k_w k_{skew} N_{ph} \frac{\Delta \varphi}{\Delta t} \tag{16}$$

where the factor k_w is winding factor, k_{skew} is the coefficient which present the skewing effects, N_{ph} is number of coil turns in series per phase winding and φ is magnetic flux.

The back-EMF of the proposed machine for different values of θ_{skew} are illustrated in Fig. 8. It is observed that the induced EMF reduces very a little. Moreover, the EMF has a small shift backward. Furthermore, Fig. 9 presents the maximum value of EMF for different skew angles. It can be seen that the maximum EMF for $\theta_{skew}=6^{\circ}$ decreases around 0.05V. II addition, harmonic analysis of EMF is performed and the results are indicated in Fig. 10. By comparing the harmonic content of the induced EMF it can be concluded that the all harmonic orders of EMF drop and it causes the EMF waveform to be smooth. Moreover, maximum EMF and EMF reduction for various θ_{skew} are compared table IV.

6. Core Losses Characteristics

One of the crucial points which has a great impact on machine performance is iron loss which should be estimated precisely. The power losses in the electrical machines consist of chiefly of three types, the magnetic losses in the magnetic circuits which is known as iron losses, the losses by joule effect in the coils which is called copper losses and the mechanical losses which is produced by friction and ventilation.

Calculating of the iron losses and the modeling of the soft magnetic materials are two completely dependent points. Thus, the hysteresis is taken into consideration at the level of the magnetic behavior law B(H), and the computation of the magnetic losses is therefore carried out directly. In addition, the hysteresis is neglected at the level of the magnetic behavior law B(H), and the computation of the magnetic losses is carried out a posteriori starting from theoretical or experimental formulas [16].

Two reputable methods are being used by machines designers to assess the iron loss such as Bertotti formula and LS (Loss Surface) model. In this paper, Bertotti formulas is used to calculate the iron losses. In this paper, the formulas of Bertotti is used to calculate the iron losses [17]-[18].

In Bertotti theory, the expression of the magnetic losses is a function of the frequency and of the peak value of the magnetic flux density and total magnetic losses (17) are

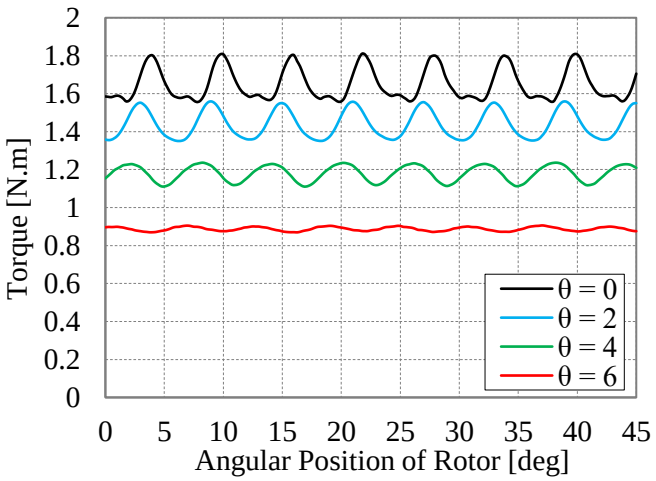

Fig. 5. FE computation of torque for different values of skew angle

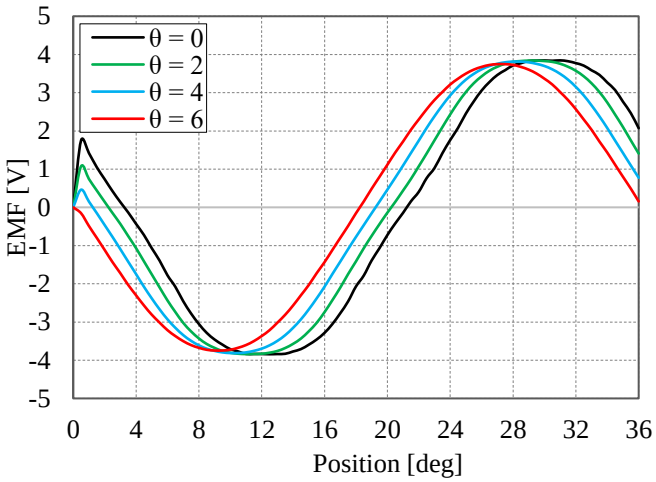

Fig. 8. FE computation of EMF of phase for different values of skew angle

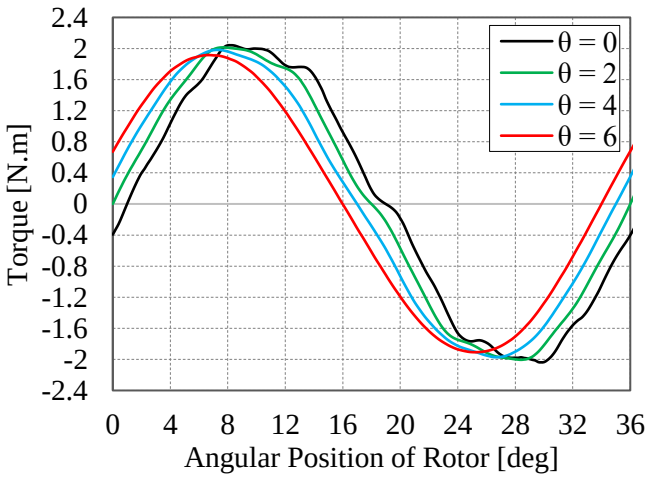

Fig. 6. FE computation of T-δ for different values of skew angle

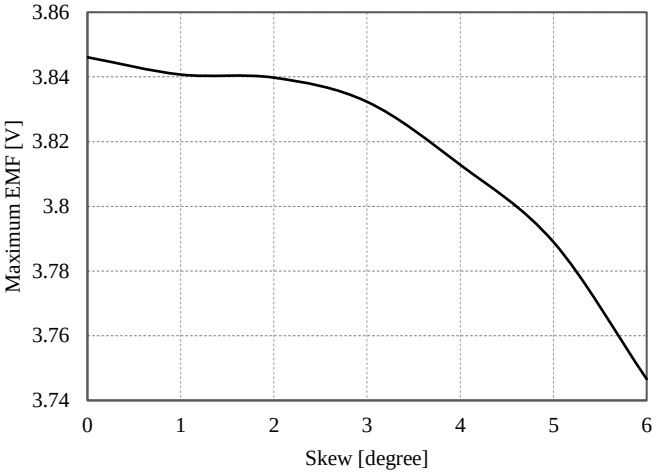

Fig. 9. Maximum induced phase EMF versus different values of skew angle

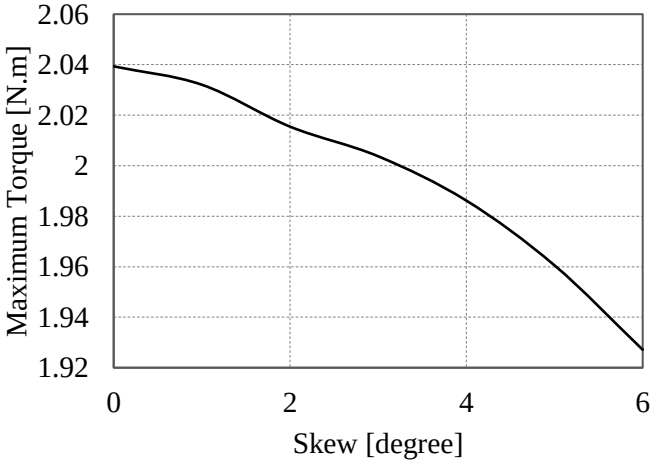

Fig. 7. Maximum torque versus different values of skew angle

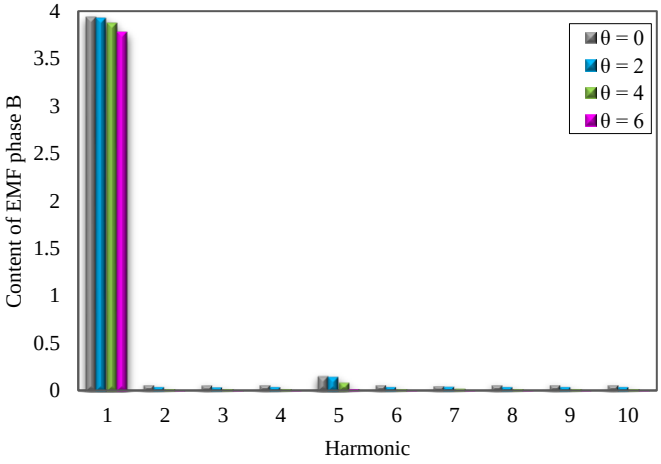

Fig. 10. Compareof harmonic content of EMF phase B calculated by FEM

Table 2: Compare of t-δ for various values of skew angle

Skew Angle	T_{Max} [N.m]	Torque Reduction [%]	T_{Cog}/T
0	2.039341	0.00%	5.43%
1	2.032071	0.36%	5.02%
2	2.015476	1.17%	3.53%
3	2.003732	1.75%	2.38%
4	1.986186	2.61%	1.58%
5	1.960552	3.86%	0.71%
6	1.927137	5.50%	0.05%

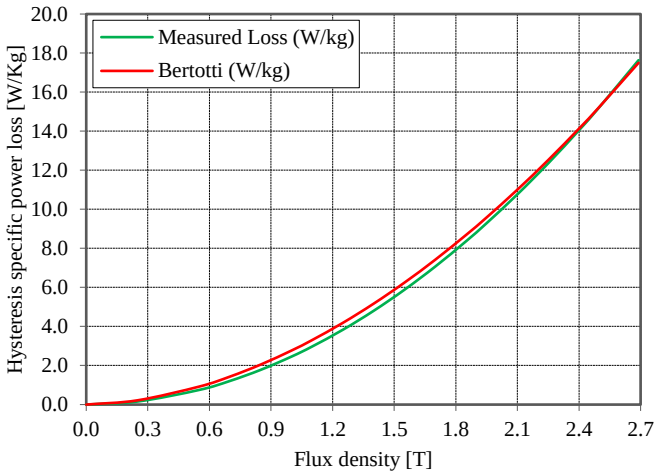

Fig. 11. Iron losses at f = 66.67Hz in M400-50A

divided into three terms, hysteresis losses (18), classical eddy currents losses (19) and excess losses (20) as follow [17]:

$$P_{Loss} = \left(P_{hys} + P_{eddy} + P_{\text{exc}}\right)k_f \quad (17)$$

$$P_{hystersis} = k_h f B_m^{\kappa} \quad (18)$$

$$P_{eddy} = \frac{\sigma \pi^2 d^2}{6}(B_m f)^2 \quad (19)$$

$$P_{\text{excess}} = k_e (B_m f)^{1.5} \quad (20)$$

where κ is the coefficient of Steinmetz, ranging from 1.6 to 2, k_f is the stacking factor which usually is very close to 1, k_e and k_e are hysteresis loss coefficient and excess loss coefficient respectively, σ is the conductivity of the material, d is the thickness of the lamination, f is machine frequency and B_m is the peak value of the magnetic flux density.

As shown in Fig. 11, the iron losses-flux density cure which is obtained by Bertotti overlaps with the measured cure perfectly. Moreover, the calculated core losses in demonstrated in Fig. 11 for θ_{skew}=1 and θ_{skew}=6. The core losses of the machine are calculated based on the formula

Table 2: Compare of EMF for various values of skew angle

Skew Angle	EMF [N.m]	EMF Reduction [%]
0	3.84608603	0.00%
1	3.840733048	0.14%
2	3.83978471	0.16%
3	3.832326401	0.36%
4	3.812842606	0.86%
5	3.788969318	1.49%
6	3.746603905	2.59%

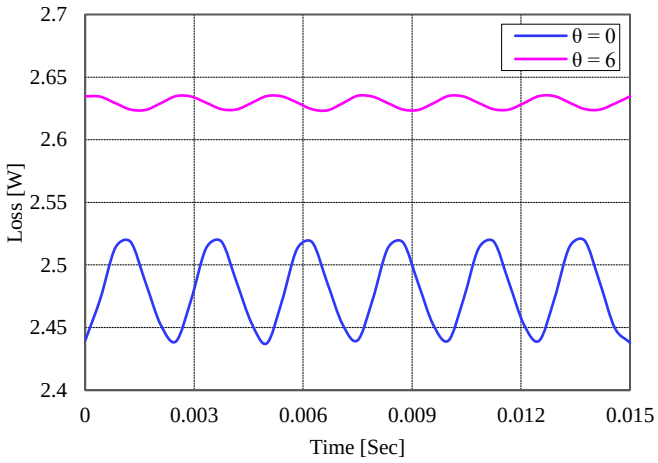

Fig. 12. Iron losses based on formulas of Bertotti

of Bertotti and presented in Fig. 12 both θ_{skew}=1 and θ_{skew}=6.

Table 2: Detail of machine iron losses

Skew Angle	Total Losses	Hysteresis Losses	Classical Losses	Excess Losses
0	2.4802	1.8138	0.378	0.28837
6	2.6293	1.9182	0.40455	0.30656

7. Conclusion

The effectiveness of rotor skewing on effective parameters of FSPM machines which have great impact on machine's performance have been investigated under different skew angles. It is found that the cogging torque can be eliminated completely by rotor skewing in FSPM machines. Also, output torque of machine falls, but the decrement of output torque is not remarkable. It should be considered that maximum output torque is depended on the position of the rotor in FSPM machines. Thus, to reach the maximum output torque, it is necessary to calculate T-δ. The effects on rotor skewing have been examined and it is found that back-EMF is being smoother with a very a little drop. Finally, the core losses of the machine for both non-skewed and skewed condition have been computed,

and it found that the core losses increased which decreases machine's efficiency. Generally, it can be concluded that rotor skewing is the best approach to improve machine's performance but some studies should be done to find the optimal skew angle and rotor position to make this study more practical.

References

[1] Z. Q. Zhu and D. Howe, "Electrical Machines and Drives for Electric, Hybrid, and Fuel Cell Vehicles," in Proceedings of the IEEE, vol. 95, no. 4, pp. 746-765, April 2007.

[2] L. Shao, W. Hua, N. Dai, M. Tong and M. Cheng, "Mathematical Modeling of a 12-Phase Flux-Switching Permanent-Magnet Machine for Wind Power Generation," in IEEE Transactions on Industrial Electronics, vol. 63, no. 1, pp. 504-516, Jan. 2016.

[3] M. Cheng, W. Hua, J. Zhang, and W. Zhao, "Overview of stator permanent magnet brushless machines," IEEE Trans. Ind. Electron., vol. 58, no. 11, pp. 5087-5101, Nov. 2011.

[4] J. Zhang, M. Cheng, Z. Chen, and W. Hua, "Comparison of stator mounted permanent-magnet machines based on a general power equation," IEEE Trans. Energy Convers., vol. 24, no. 4, pp. 826-834, Dec. 2009.

[5] Wei Hua; Ming Cheng; Gan Zhang, "A Novel Hybrid Excitation Flux-Switching Motor for Hybrid Vehicles," in Magnetics, IEEE Transactions on, vol.45, no.10, pp.4728-4731, Oct. 2009.

[6] J. Ojeda, M. G. Simoes, G. Li, M. Gabsi "Design of a Flux-Switching Electrical Generator for Wind Turbine Systems," in IEEE Transaction on Industry Application, Vol. 48, No. 6, pp. 1808–1816, 2012.

[7] Wei Hua; Ming Cheng; Zhu, Z.Q.; Howe, D., "Design of Flux-Switching Permanent Magnet Machine Considering the Limitation of Inverter and Flux-Weakening Capability," Industry Applications Conference, 2006. 41st IAS Annual Meeting. Conference Record of the 2006 IEEE, vol.5, no., pp.2403-2410, 8-12 Oct. 2006.

[8] Sulaiman, E.; Kosaka, T.; Matsui, N., "Design optimization of 12Slot-10Pole hybrid excitation flux switching synchronous machine with 0.4kg permanent magnet for hybrid electric vehicles," Power Electronics and ECCE Asia (ICPE & ECCE), 2011 IEEE 8th International Conference on, vol., no., pp.1913-1920, May 30 2011-June 3 2011.

[9] Zhu, Z.Q.; Pang, Y.; Howe, D.; Iwasaki, S.; Deodhar, R.; Pride, A., "Analysis of electromagnetic performance of flux-switching permanent magnet Machines by nonlinear adaptive lumped parameter magnetic circuit model," Magnetics, IEEE Transactions on , vol.41, no.11, pp.4277-4287, Nov. 2005.

[10] Zhu, Z.Q.; Pang, Y.; Howe, D.; Iwasaki, S.; Deodhar, R.; Pride, A., "Analysis of electromagnetic performance of flux-switching permanent magnet Machines by nonlinear adaptive lumped parameter magnetic circuit model," Magnetics, IEEE Transactions on , vol.41, no.11, pp.4277-4287, Nov. 2005.

[11] J. X. Shen and W. Z. Fei, "Permanent magnet flux switching machines — Topologies, analysis and optimization," Power Engineering, Energy and Electrical Drives (POWERENG), 2013 Fourth International Conference on, Istanbul, 2013, pp. 352-366.

[12] Zhu, Z.Q.; Thomas, A.S.; Chen, J.T.; Jewell, G.W., "Cogging Torque in Flux-Switching Permanent Magnet Machines," IEEE Transactions on Magnetics, vol.45, no.10, pp.4708-4711, Oct. 2009.

[13] W. Fei, P. C. K. Luk and J. Shen, "Torque Analysis of Permanent-Magnet Flux Switching Machines With Rotor Step Skewing," in IEEE Transactions on Magnetics, vol. 48, no. 10, pp. 2664-2673, Oct. 2012.

[14] N. Bianchi and S. Bolognani, "Design techniques for reducing the cogging torque in surface-mounted PM motors," in *IEEE Transactions on Industry Applications*, vol. 38, no. 5, pp. 1259-1265, Sep/Oct 2002.

[15] C. Sikder, I. Husain and W. Ouyang, "Cogging Torque Reduction in Flux-Switching Permanent-Magnet Machines by Rotor Pole Shaping," in IEEE Transactions on Industry Applications, vol. 51, no. 5, pp. 3609-3619, Sept.-Oct. 2015.

[16] T. Chevalier, "A new dynamic hysteresis model for electrical steel sheet", Phys. B: Phys. Condens. Matter, vol. 275/13, pp. 197-201, 2000

[17] G. Bertotti, F. Fiorillo, G. Soardo, "The Prediction of Power Losses In Soft Magnetic Materials," Journal de Physique Colloques, 1988, 49 (C8), pp.C8-1915-C8-1919.

[18] F. Fiorillo and A. Novikov, "An improved approach to power losses in magnetic laminations under nonsinusoidal induction waveform," in IEEE Transactions on Magnetics, vol. 26, no. 5, pp. 2904-2910, Sep 1990.